NEW CONCEPT OF SCATTERED RADIATION IMAGING WITH HIGH SENSITIVITY

M. K. Nguyen and G. Fourreau

Equipes Traitement des Images et du Signal (ETIS)
CNRS 8051/ ENSEA / Université de Cergy-Pontoise
6 avenue du Ponceau,
95014 Cergy-Pontoise Cedex, France

T. T. Truong and C. Driol

Laboratoire de Physique Théorique et Modélisation (LPTM)
CNRS 8089/ Université de Cergy-Pontoise
2 rue Adolphe Chauvin,
95302 Cergy-Pontoise Cedex, France

ABSTRACT

We propose a new scheme for imaging radiation emitting objects by measuring its non collimated scattered radiation at various energies. A few years ago we have put forward the idea of scatter imaging and show how it works with a collimated detector. To increase drastically the sensitivity of this modality as well as its field of view and resolution we propose that data acquisition should be performed without collimation as it is done in Compton cameras. We discuss image formation by scattered radiation in this context by computing and comparing the related Point Spread Functions (PSF) and comment on their properties. We also present numerical simulations to support the attractiveness of this modality.

Index Terms— Biomedical imaging, nuclear imaging, gamma rays, scattering, sensitivity

1. INTRODUCTION

Scattered radiation in emission imaging has appeared as one of the promising contenders for future active imaging agent in nuclear medicine [1, 2, 3, 4, 5, 6, 7]. Conventional three dimensional techniques have so far relied on non scattered or primary radiation and treated scattered radiation as noise and perturbing factor which must be eliminated as much as possible. However since the fifties, there has been a continuous interest in Compton scattered radiation and its possible usage for tomography or three dimensional imaging [8, 9, 10, 11]. Numerous proposals have been made in this direction. Most devices use collimated point sources of gamma rays scanning the electronic density inside matter and the scattered radiation is registered by a movable point-like detector outside, e.g. [12]. On the other hand, a valuable idea to exploit scattered radiation in emission imaging is the concept of electronic collimation for gamma camera [13], introduced about two decades ago.

Recently we have put forward the idea of exploiting information encoded in scattered radiation but detected by a standard gamma camera with collimator [3]. We have also shown that three dimensional reconstruction is possible since an analytic inversion formula exists, at least when attenuation is neglected and the electronic density of the scattering medium roughly constant. But using a collimator means that a huge amount of scattered rays are discarded (only $1/10000$ part of the emitted radiation reaches the detector). Therefore we take now the bold step to remove entirely the collimator of the gamma camera. Our operating modality is nevertheless different from that of a Compton camera since it does not make use of coincidence detection.

Fig. 1 shows how single scattered radiation is used in image formation with and without collimator. How scattered radiation works in the two cases is displayed in Fig. 2 and Fig. 3. The removal of the collimator allows a detection site to register many more contributions arriving from all possible directions in the upper half space of the detector. To focus on the essentials of image formation and convey first the interesting aspects, we choose to present the computations in two dimensions since they are less involved. Section 2 describes the successive steps of image formation. In section 3, we establish the analytical expressions of the Point Spread Function (PSF) in the two cases and compare them. Finally in section 4 we present numerical simulation results which support the possible implementation of this new imaging principle. Conclusion and perspectives are in the last section.

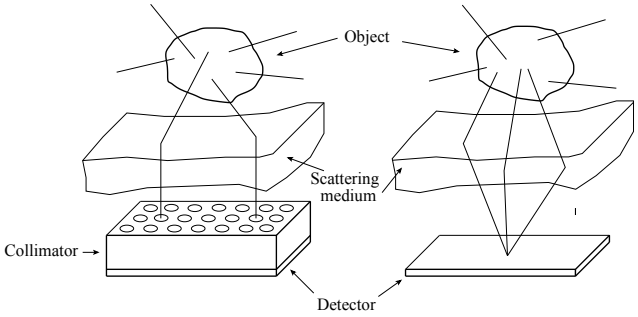

Fig. 1. Two modalities in emission scattered radiation imaging.

2. SCATTERED RADIATION IMAGE FORMATION WITHOUT COLLIMATION

Let

$\mathbf{S} = (x_S, y_S)$ be a radiation emitting point source of an object represented by its activity density $f(\mathbf{S})$, a real valued non negative function, compactly supported,

$\mathbf{M} = (x_M, y_M)$, a scattering site inside the surrounding medium, which eventually may include the object itself,

$\mathbf{D} = (x_D, 0)$, a detection site on the linear detector.

The detected radiation at $\mathbf{D}$ has undergone at least one Compton scattering. Its energy E, after collision, is related to the scattering angle ω by the Compton relation:

$$E = E_0 \frac{1}{1 + \varepsilon(1 - \cos\omega)}, \tag{1}$$

where E_0 is the photon initial energy, $\varepsilon = E_0/mc^2$ and mc^2 the rest energy of the electron. The Compton effect is thought to have

establish the particle aspect of radiation known as photon.

To see the role of scattered radiation in this new imaging principle, we shall adopt the following simplifying hypothesis in the computation:

- since single Compton scattering are dominant, only these events will be considered hereafter. Higher order scattering will be the object of future work,
- radiation attenuation in medium will be neglected,
- the medium electronic density is assumed to be approximately constant, i.e. $n_e = \text{const}$,
- the primary emission by an object point source $\mathbf{S}$ is assumed to be isotropic.

The image recorded by the detector appears then as the photon flux density $g(\mathbf{D}, \omega)$ at site $\mathbf{D}$ and at given scattered photon energy E, or equivalently at scattering angle ω. Its expression can be obtained by following the photon path from emission to detection with one scattering at site $\mathbf{M}$. Generally $g(\mathbf{D}, \omega)$ appears as a linear integral transform of the activity density $f(\mathbf{S})$:

$$g(\mathbf{D}, \omega) = \int d\mathbf{S}\, f(\mathbf{S}) \mathcal{P}(\mathbf{D}, \omega | \mathbf{S}), \tag{2}$$

as we shall see in the following.

Because the primary emission is isotropic, the photon flux density emitted at $\mathbf{S}$ and reaching a scattering site $\mathbf{M}$ of small transverse dimension (e.g. diameter) e, is

$$\frac{f(\mathbf{S}) d\mathbf{S}}{2\pi} \arctan\left(\frac{e}{SM}\right) \frac{1}{e}.$$

This number of photons will scatter with $n_e(\mathbf{M}) d\mathbf{M}$ electrons at site $\mathbf{M}$ and will be deflected by an angle ω from its initial direction with a probability $r_e\, P(\omega)$, the Compton differential cross section in two dimensions per scatterer. Hence the scattered photon density reaching detection site $\mathbf{D}$ is

$$\frac{f(\mathbf{S}) d\mathbf{S}}{2\pi} \arctan\left(\frac{e}{SM}\right) \frac{1}{e^2} n_e(\mathbf{M}) d\mathbf{M}\, r_e\, P(\omega) \arctan\left(\frac{e}{MD}\right).$$

The totality of detected photons is thus the integral over all emission sites $\mathbf{S}$ and all scattering sites $\mathbf{M}$ such that $\overrightarrow{SM}$ makes an angle ω with $\overrightarrow{MD}$. This is exactly what Eq. (2) expresses.

3. POINT SPREAD FUNCTION (PSF)

$\mathcal{P}(\mathbf{D}, \omega | \mathbf{S})$ is by definition the image of a unit single point source at $\mathbf{S}$. The scattering condition under scattering angle ω means that the scattering site $\mathbf{M}$ must be on two arcs of circles subtending an angle $(\pi - \omega)$ passing through sites $\mathbf{D}$ and $\mathbf{S}$ (see Fig. 3). Thus the PSF is given by an integral over two arcs of circle

$$\mathcal{P}(x_D, \omega | x_S, y_S) = K(\omega) \frac{1}{e^2} \times \int_{\mathbf{M} \in \text{Arcs}} \arctan\left(\frac{e}{SM}\right) \arctan\left(\frac{e}{MD}\right) d\mathbf{M}, \tag{3}$$

with $K(\omega) = n_e\, r_e\, P(\omega)/2\pi$, and $n_e = n_e(\mathbf{M})$.

For computation we choose polar coordinates such that $\mathbf{S} = (d, \alpha)$, with $DS = d$ and $\mathbf{M} = (r, \theta)$, with $DM = r$ and $\overrightarrow{DM} \cdot \overrightarrow{DS} = r\, d\, \cos\gamma$.

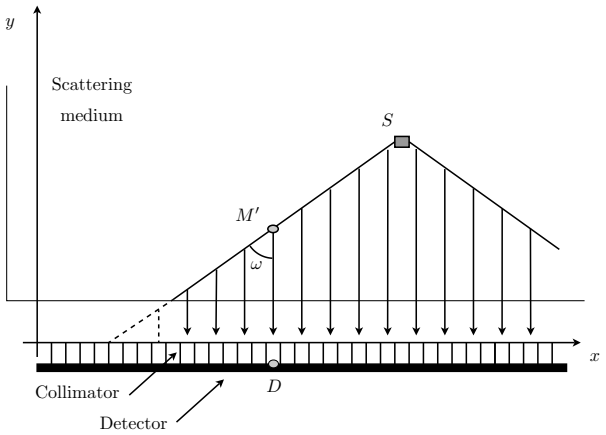

Fig. 2. Coordinates for scatter image formation with collimator

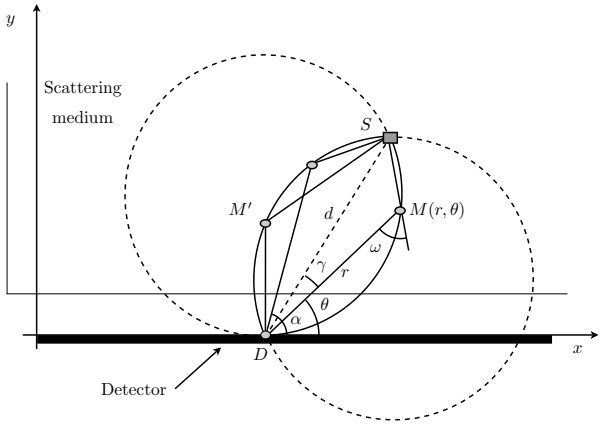

Fig. 3. Coordinates for scatter image formation without collimator

The circular arcs have polar equations

$$r = d\, \frac{\sin(\omega - \gamma)}{\sin\omega} \quad \text{and} \quad r = d\, \frac{\sin(\omega + \gamma)}{\sin\omega}, \tag{4}$$

where γ is the angle between $\overrightarrow{DS}$ and $\overrightarrow{DM}$: $\gamma = (\theta - \alpha)$.

The distance SM can be extracted from a simple identity in the triangle DSM, i.e.

$$SM = d\, \frac{\sin\gamma}{\sin\omega}.$$

The integration element $d\mathbf{M}$ corresponds to a small area delimited by a portion of the arc of circle and by e

$$d\mathbf{M} = e\, \frac{d}{\sin\omega}\, d\gamma.$$

As the scattering medium is of finite extent, the lower limits of integration should be calculated beforehand, this depends on ω and will be noted $\gamma_l(\omega)$

$$\mathcal{P}(x_D, \omega) = K(\omega) \frac{d}{e \sin\omega} \sum_{\text{Arcs}} \int_0^{\gamma_l(\omega)} \arctan\left(\frac{e \sin\omega}{d \sin\gamma}\right) \times \arctan\left(\frac{e \sin\omega}{d \sin(\omega - \gamma)}\right) d\gamma. \tag{5}$$

In reality to account for the structure of a linear detector a factor $\sin(\alpha-\gamma)$ should be added to the integrand in the second $\arctan$ of Eq. (5) to describe the projection of the scattered photon flux density on this detector.

Now if a collimator is mounted on the detector (see Fig. 2) then only one scattering site $\mathbf{M}$, located on the perpendicular to the detector at site $\mathbf{D}$, will contribute to detection site $\mathbf{D}$. Thus the integration is restricted by a delta function which picks out only the corresponding value of γ, i.e. $\gamma_0 = (\pi/2 - \alpha)$. Consequently the PSF in the presence of a collimator has the expression

$$\mathcal{P}_{coll}(x_D,\omega) = K(\omega)\frac{d}{e\sin\omega}\arctan\left(\frac{e\sin\omega}{d\sin\gamma}\right)$$

$$\times\ \arctan\left(\frac{e\sin\omega}{d\sin(\omega-\gamma)}\right)\Delta\gamma \qquad (6)$$

The angular element $\Delta\gamma$ should in practice correspond to the smallest step in the discretization of the circular arc in numerical calculations. Once it is fixed, one can compare the two PSF curves. Fig. 4 and Fig. 5 show the PSF curves in the two cases for different scattering angles, the horizontal axis being the Ox axis of the receiving face of the detector.

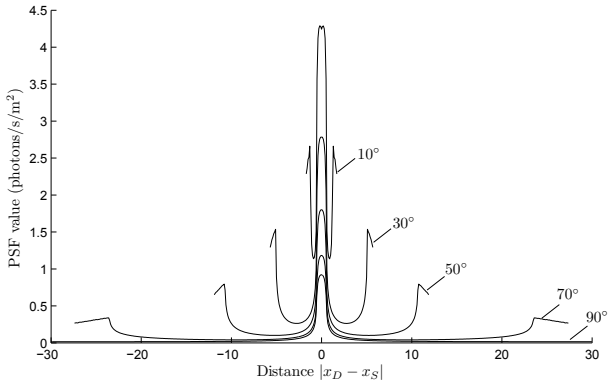

Fig. 4. PSF curves at various scattering angles with collimator

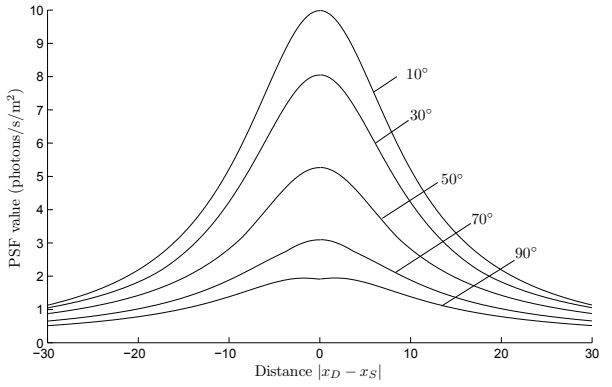

Fig. 5. PSF values at various scattering angles without collimator

As an illustrative example, let us consider the case of a scattering angle of 50 degrees, the signal without collimator is on the average 20.2 stronger than the one with collimator. This can be seen on the PSF profiles in Fig. 6. Thus image formation without collimator comes out with much higher sensitivity as shown by color level display in Fig. 7.

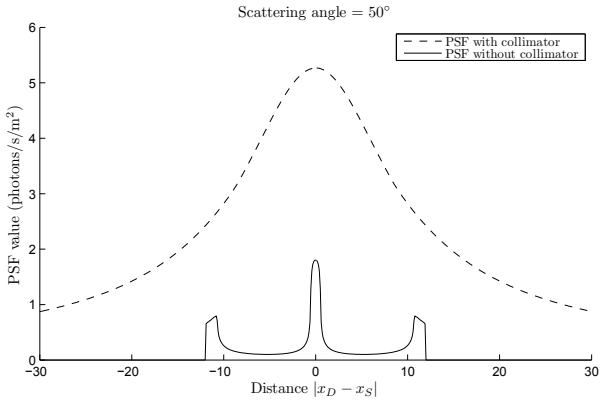

Fig. 6. Comparison of PSF images on the detector: with collimator (filled line) and without collimator (dotted line)

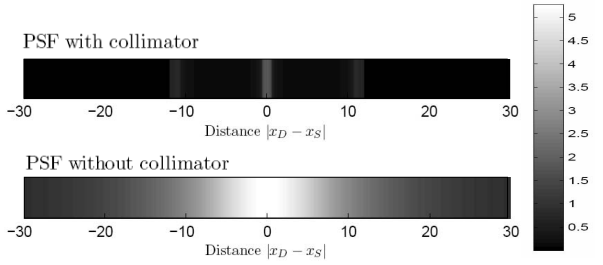

Fig. 7. Comparison of sensitivity on the detector: with collimator (upper short line) and without collimator (lower long line)

4. NUMERICAL SIMULATION RESULTS

In this section, we present the results of two numerical reconstruction of the Shepp-Logan medical phantom (see Fig. 8 for the original image). The scattering medium is discretized with 55 points along the x and y axis. The detector line is placed on the line $y = 0$.

The photon flux density coming from the object and arriving on the detector is simulated using Eqs. (5) or (6). The images simulated without collimator are on the average 15 to 30 times more sensitive than those with collimator.

Then, we construct the weight matrix of the medium by calculating, for each point of the mesh, the PSF on the detector at different scattering angles. The reconstruction is carried out by inverting the weight matrix using the Singular Value Decomposition method.

Fig. 9 shows the result when a collimator is mounted on the detector. We can see that the part of the object near the detector is better reconstructed than the upper part of the image. The three small structures are invisible. The reconstruction relative error is $9.13\ \%$. On the other hand, when we simulate a detector without collimator

(Fig. 10), the whole image is correctly reconstructed: the relative error is $1.17\ 10^{-4}$ %. The results are very encouraging and push us to explore further this new imaging principle.

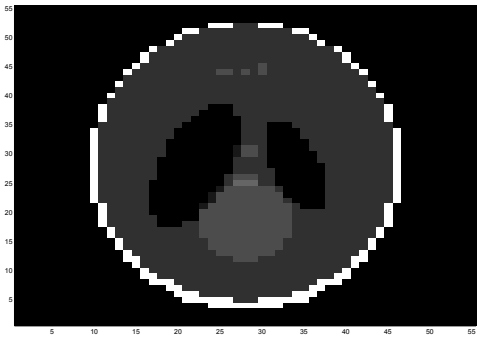

Fig. 8. Original Shepp-Logan phantom

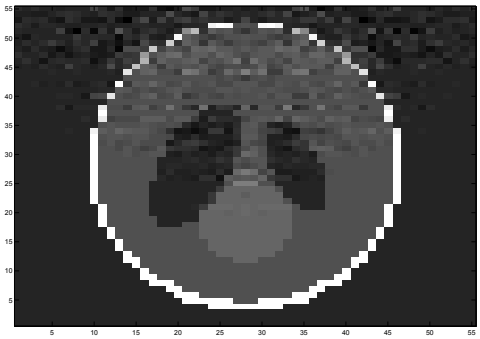

Fig. 9. Shepp-Logan phantom reconstruction with collimator

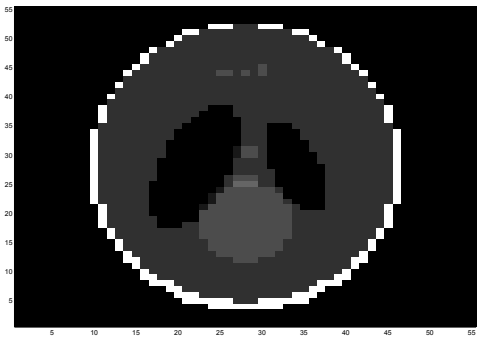

Fig. 10. Shepp-Logan phantom reconstruction without collimator

5. CONCLUSION AND PERSPECTIVE

These promising results open the way to a new concept of high sensitivity imaging system which may find applications in fields beyond biomedical imaging such as industrial non destructive control, high energy astrophysics, environmental survey, etc. The transition from two dimensional imaging to three dimensional imaging, and the analytical inversion of the PSF - a major mathematical challenge - are topics for future research.

6. REFERENCES

[1] P.C. Johns, R.J. Leclair, and M.P. Wismayer, "Medical x-ray imaging with scattered photons," in *Opto-Canada: SPIE Regional Meeting in Optoelectronics, Photonics and Imaging, SPIE* **TD 01**, Ottawa, Canada, May 2002, pp. 355–357.

[2] M.K. Nguyen and T. T. Truong, "Exact inversion of a compound conical radon transform and a novel nuclear imaging principle," *C. R. Acad. Sci. Paris Ser. I*, vol. 335, pp. 213–217, 2002.

[3] M.K. Nguyen and T.T. Truong, "On an integral transform and its inverse in nuclear imaging," *Inverse Problems*, vol. 18, pp. 265–277, 2002.

[4] M.K. Nguyen, T.T. Truong, and H.D. Bui, "A novel inverse problem in medical emission imaging," in *4th International Conference on Inverse Problems in Engineering: Theory and Practice*, Rio de Janeiro, Brazil, May 2002, pp. 397–404.

[5] M.K. Nguyen, T.T. Truong, and J.L. Delarbre, "Physical analysis of scattered radiation and a new object reconstruction in photon imaging systems," in *Int. Conf. Physics in Signal and Image Processing*, Grenoble, France, January 2003, pp. 209–212.

[6] M.K. Nguyen, T.T. Truong, H.D. Bui, and J.L. Delarbre, "A novel inverse problem in gamma-ray emission imaging," *Journal of Inverse Problems in Science and Engineering*, vol. 12, pp. 225–246, 2004.

[7] J. L. Delarbre, M.K. Nguyen, and T.T. Truong, "Towards a novel dual-modality imaging using scattered radiation," in *ICASSP 2006*, Toulouse, France, May 2006.

[8] R. L. Clarke, E. N. C. Milne, and G. Van Dyk, "The use of compton scattered gamma rays for tomography," *Inv. Radiology*, vol. 11, pp. 225–235, 1976.

[9] B. Bridge, F. Harirchian, D. C. Imrie, Y. Mehrabi, and A. R. Meragi, "Experiments in compton scatter imaging of materials with wide-ranging densities using a low-activity gamma source," *NDT International*, vol. 20, pp. 339–346, 1987.

[10] E.M.A. Hussein, "Compton scatter imaging systems," in *Bioinstrumentation: Research, Developments and Applications*, Donald L. Wise, Ed., chapter 35, pp. 1053–1086. Butterworths, 1990.

[11] B. L. Evans, J. B. Martin, L. W. Burggaf, and M. C. Roggemann, "Nondestructive inspection using compton scatter tomography," *IEEE Transactions on Nuclear Science*, vol. 45, no. 3, June 1998.

[12] S.J. Norton, "Compton scattering tomography," *J. Appl. Phys.*, vol. 76, no. 4, pp. 2007–2015, 1994.

[13] M. Singh, "An electronically collimated gamma camera for single photn emission computed tomography. part i: Theoretical considerations and design criteria.," *Med. Phys.*, vol. 10, pp. 421–427, 1983.